doi:10.1246/cl.2011.837
Published on the web July 16, 2011

Shape-controlled Synthesis of $LiMnPO_4$ via a Hydrothermal Route and Its Electrochemical Behavior in Lithium Ion Batteries

Ting Li,[1] Tao Mei,[1] Yongchun Zhu,*[1] Huaxu Gong,[1] Tao Huang,[1] and Yitai Qian*[1,2]
[1]*Hefei National Laboratory for Physical Science at Microscale and Department of Chemistry, University of Science and Technology of China, Hefei, Anhui 230026, P. R. China*
[2]*Key Laboratory of Colloid and Interface Chemistry, Ministry of Education, and School of Chemistry and Chemical Engineering, Shandong University, Jinan 250100, P. R. China*

(Received May 19, 2011; CL-110426; E-mail: ytqian@ustc.edu.cn)

$LiMnPO_4$ nanosquares with the edge size of 800–1000 nm and the thickness of 50–250 nm were hydrothermally prepared using 1.0 g of $Na_4P_2O_7 \cdot 10H_2O$. Subsequently, the $LiMnPO_4$ nanosquares were annealed with ascorbic acid (Vc) at 600 °C to prepare the $LiMnPO_4$/C nanocomposites. The electrochemical performances of $LiMnPO_4$ and $LiMnPO_4$/C at 0.1 C demonstrated first run discharge capacities at 81.6 and 125.5 mA h g^{-1}, respectively. In addition, spindles, bows, and cubes composed of $LiMnPO_4$ nanosquares have also been prepared.

$LiMnPO_4$ could be an excellent candidate for a new cathode material owing to its redox potential of ca. 4.1 V vs. Li^+/Li, the theoretical energy density (697 W h kg^{-1} = 170 mA h g^{-1} × 4.1 V) is 1.2 times larger than that of $LiFePO_4$ (578 W h kg^{-1} = 170 mA h g^{-1} × 3.4 V), and the use of well-known electrolytes such as propylene carbonate (PC), ethylene carbonate (EC), and dimethoxyethane (DME) are suitable for $LiMnPO_4$.[1]

Various synthetic routes have been applied to prepare $LiMnPO_4$, such as molten hydrocarbon-assisted solid-state reaction,[2] direct precipitation,[3] sol–gel method,[4] polyol method,[5] ultrasonic spray pyrolysis,[6,7] combination of spray pyrolysis,[8,9] supercritical ethanol process,[10] ionothermal,[11] solvethermal,[12,13] carbothermal reduction,[14] microwave hydrothermal,[15] and hydrothermal methods.[16,17] $LiMnPO_4$ nanoplates with a thickness of ca. 50 nm were prepared via a molten hydrocarbon-assisted solid-state reaction, which present first-run discharge capacities of 168 mA h g^{-1} at 0.02 C and 117 mA h g^{-1} at 1 C.[2] Platelet $LiMnPO_4$ particles of 25–30 nm were synthesized by a novel polyol method, which showed first-run discharge capacities of 145 mA h g^{-1} at 0.05 C, 141 mA h g^{-1} at 0.1 C, and 113 mA h g^{-1} at 1 C.[5] The hexagonal prism and anomalous nanoplates $LiMnPO_4$ were obtained by a hydrothermal route, which showed first-run discharge capacities of ca. 32 and ca. 48 mA h g^{-1} at 5 mA g^{-1}.[17]

In this study, $LiMnPO_4$ nanosquares with the edge size of 800–1000 nm and the thickness of 50–250 nm were hydrothermally prepared using 1.0 g of $Na_4P_2O_7 \cdot 10H_2O$. Subsequently, the $LiMnPO_4$ nanosquares were annealed with ascorbic acid (Vc) at 600 °C to prepare the $LiMnPO_4$/C nanocomposites. The electrochemical performances of $LiMnPO_4$ and $LiMnPO_4$/C at 0.1 C demonstrated first run discharge capacities at 81.6 and 125.5 mA h g^{-1}, respectively. The $LiMnPO_4$/C maintained a stable discharge capacity at 108.8 mA h g^{-1} after 50 cycles under 0.1 C. In addition, spindles, bows, and cubes composed of nanosquares have also been prepared varying the amount of $Na_4P_2O_7 \cdot 10H_2O$. Their electrochemical capacities were lower than the $LiMnPO_4$ nanosquares, and we found the capacities increased with the decrease of size of the as-prepared $LiMnPO_4$.

All reagents were analytical grade and were purchased from Shanghai Chemical Industrial Corp. and used without further purification. In a typical procedure, 0.245 g of $MnC_2O_4 \cdot 4H_2O$, 1.0 g of $Na_4P_2O_7 \cdot 10H_2O$, 0.126 g of $LiOH \cdot H_2O$, and 0.115 g of H_3PO_4 were dissolved in 50 mL of distilled water. The $MnC_2O_4 \cdot 4H_2O$ and $Na_4P_2O_7 \cdot 10H_2O$ were mixed first, and then LiOH was added. After the addition of H_3PO_4, a brown gel formed in the beaker. The resulting gel was transferred into a 60-mL capacity Teflon-lined stainless steel autoclave. The autoclave was heated at 180 °C for 24 h. After cooling to room temperature, the precipitated product was filtered off and washed several times with distilled water and anhydrous ethanol. Thereafter, the products were dried at 60 °C for 3 h in a vacuum oven.

The phase identification of the products was accomplished using powder X-ray diffraction (XRD), employing a Philips X'pert X-ray diffractometer with Cu Kα radiation (λ = 1.54178 Å). A scan rate of 0.05° s^{-1} was applied to record the pattern in the 2θ range of 15–60°. The scanning electron microscopy (SEM) images were taken by using a JEOL-JSM-6700F field-emitting (FE) scanning electron microscope.

Figure 1a shows the XRD pattern of the product prepared with 1.0 g of $Na_4P_2O_7 \cdot 10H_2O$. All diffraction peaks could be clearly indexed as olivine-type $LiMnPO_4$ with space group of *Pmnb* of the orthorhombic system (JCPDS No. 74-0375). No obvious peak is observed for other impurities. Figure 1b exhibits the low-resolution SEM image of the product, which presents the shape of nanosquares. The product consists of almost all of such uniform nanosquares, giving the information that high yield and good dispersant can be readily achieved through this route. Figure 1c exhibits the high-resolution SEM image of nanosquares. It clearly shows that the average length and the thickness of these nanosquares are 800–1000 and 50–250 nm, respectively.

In addition, spindles, bows, and cubes composed of nanosquares have also been prepared varying the amount of $Na_4P_2O_7 \cdot 10H_2O$ from 0 to 0.4 g. Figure 2 shows the XRD patterns of the products prepared with different amounts of $Na_4P_2O_7 \cdot 10H_2O$. All the peaks can be identified as $LiMnPO_4$ with orthorhombic phase (JCPDS No. 74-0375).

Figure 3 shows the SEM images of the products prepared with different amounts of $Na_4P_2O_7 \cdot 10H_2O$. Figures 3a and 3b are SEM images of the sample prepared without $Na_4P_2O_7 \cdot 10H_2O$, which show spindle $LiMnPO_4$ structure with a mean length of 4 μm and a width in the range of ca. 0.8 μm. The spindles are composed of nanosquares with thickness of 100–200 nm and length of 500–800 nm. Figures 3c and 3d are SEM images of the $LiMnPO_4$ prepared with 0.2 g of $Na_4P_2O_7 \cdot 10H_2O$,

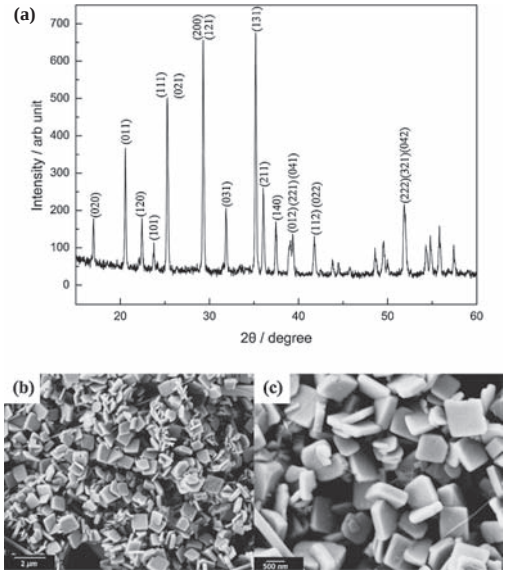

Figure 1. XRD pattern and SEM of $LiMnPO_4$ prepared with 1.0 g of $Na_4P_2O_7 \cdot 10H_2O$.

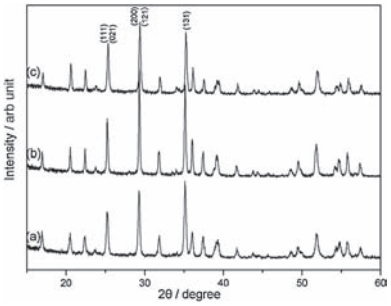

Figure 2. XRD patterns of $LiMnPO_4$ prepared with different amounts of $Na_4P_2O_7 \cdot 10H_2O$. (a) 0, (b) 0.2, and (c) 0.4 g.

which show bow $LiMnPO_4$ structure with a mean length of ca. 8 μm and a width in the range of 4 μm. While 0.4 g of $Na_4P_2O_7 \cdot 10H_2O$ added, $LiMnPO_4$ cubes composed of nanosquares (Figures 3e and 3f) were attained. The microcrystals reveal the cubic shape composed of nanosquares with the average edge length of approximately 2 μm. It can be noted that the length of the bow structures (Figure 3c) is eight times as long as the cubic microstructures (Figure 3e), and the bow structures is double the width of the cubes composed of nanosquares (Figure 3e).

It is thought that $Na_4P_2O_7 \cdot 10H_2O$ plays a significant role in the shape control of the products. The white precipitates, which were attained from the reaction of $Na_4P_2O_7 \cdot 10H_2O$ with different amounts and $MnC_2O_4 \cdot 4H_2O$ for 0.5 h at room temperature, were investigated by SEM. Without $Na_4P_2O_7 \cdot 10H_2O$, $LiMnPO_4$ gathered spontaneously into spindle block with a mean length of 4 μm and a width in the range of 0.8–1 μm (Figures 3a and 3b). While adding 0.2 g of $Na_4P_2O_7 \cdot 10H_2O$, the pH value of the solution 7.03, the precursors gathered into large irregular blocks (Figure S(a), Electronic Supporting Information; ESI[21]). Doubling the amount of $Na_4P_2O_7 \cdot 10H_2O$ (pH 9.75), it is seen that the precursors change into flakes with thickness of ca. 200 nm and length of ca. 5 μm (Figure S(b), ESI[21]). Increasing $Na_4P_2O_7 \cdot 10H_2O$ futher, the pH value of the solution being 10.20, nanobelts precursors were attained (Figure S(c), ESI[21]).

$$2Mn^{2+} + P_2O_7^{4-} = Mn_2P_2O_7$$

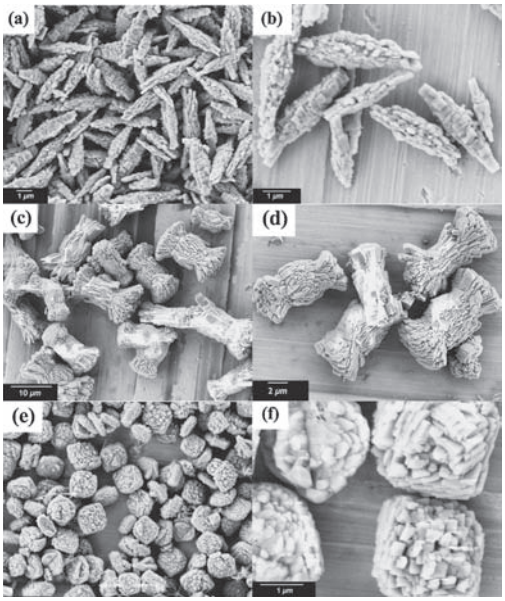

Figure 3. SEM of $LiMnPO_4$ prepared with different amounts of $Na_4P_2O_7 \cdot 10H_2O$. (a, b) 0, (c, d) 0.2, and (e, f) 0.4 g.

It is well known that aqueous $Na_4P_2O_7$ solution is alkaline, and that $P_2O_7^{4-}$ can react with Mn^{2+}. The reaction equation is as follows:

$$2Mn^{2+} + P_2O_7^{4-} = Mn_2P_2O_7 \quad (1)$$

In comparison with the stoichiometric $Mn_2P_2O_7$, while Mn^{2+} was in excess, $Na_4P_2O_7 \cdot 10H_2O$ functioned as a bridge among Mn^{2+} and made the as-prepared $LiMnPO_4$ agglomerates to the bow shape (Figures 3c and 3d). By the increase of $Na_4P_2O_7 \cdot 10H_2O$ in water, it is obvious that the as-prepared $LiMnPO_4$ disperses step by step. When 0.4 g of $Na_4P_2O_7 \cdot 10H_2O$ added in this work, a little excessive $Na_4P_2O_7 \cdot 10H_2O$ provides $P_2O_7^{4-}$, which will cover the surface of the precipitates and make them transform from blocks (Figure S(a), ESI[21]) to flakes (Figure S(b), ESI[21]), thereby the as-prepared $LiMnPO_4$ breaks up into cubes composed of nanosquares (Figures 3e and 3f). Increasing the concentration of $Na_4P_2O_7 \cdot 10H_2O$ in water, the sufficient $Na_4P_2O_7 \cdot 10H_2O$ provides ample $P_2O_7^{4-}$ to reach a significant particle surface coverage, and sufficient $P_2O_7^{4-}$ provides a dispersant steric layer that was enough to prevent extensive particle agglomeration.[18] With this, monodispersant $LiMnPO_4$ nanosquares (Figures 1b and 1c) were obtained.

$LiMnPO_4$ has been studied as cathode material for lithium ion batteries. Here, the electrochemical performance of the prepared $LiMnPO_4$ was preliminarily evaluated using a 2032 coin-type cell. Figure 4 shows the first run discharge curves of as-prepared $LiMnPO_4$ cycled between 2.5 and 4.9 V at a current density of 0.1 C. As can be seen in Figure 4, the as-prepared $LiMnPO_4$ exhibited a plateau around 4.1 V vs. Li/Li^+, which was the typical redox potential of Mn(II) $\rightleftarrows$ Mn(III) in olivine manganese phosphate. $LiMnPO_4$ spindle, bow, and cube composed of nanosquares demonstrated the reversible capacity

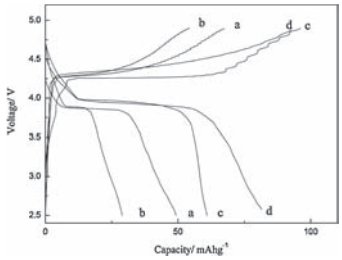

Figure 4. The charge–discharge curves of our micro-/nano-$LiMnPO_4$ at 0.1 C at room temperature: (a) $LiMnPO_4$ spindles composed of nanosquares, (b) $LiMnPO_4$ bows composed of nanosquares, (c) $LiMnPO_4$ cubes composed of nanosquares, and (d) $LiMnPO_4$ nanosquares.

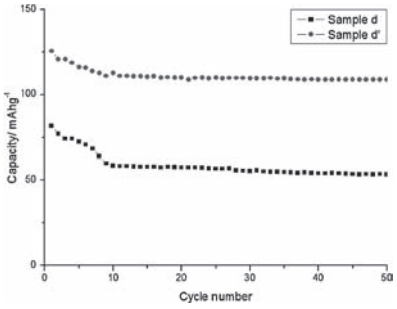

Figure 5. Cycling stability of Li/$LiMnPO_4$ (Sample d) cell and Li/$LiMnPO_4$/C (Sample d′) cell at 0.1 C at room temperature.

of 49.2, 29, and 60.9 mA h g^{-1} respectively. At room temperature, $LiMnPO_4$ nanosquares showed the first-run discharge capacities at 81.6 mA h g^{-1} at 0.1 C. For above-mentioned data, we can draw that the overall capacities of monodispersant $LiMnPO_4$ nanosquares are bigger than other microstructured $LiMnPO_4$ composed of nanosquares.

The unsatisfactory reversible capacities of $LiMnPO_4$ result from its poor inherent electronic conductivity. According to previous reports, $LiMnPO_4$ modified by carbon has an obvious effect on enhancing its capacity. Citric acid and sucrose,[6] carbon black,[19] acetylene black,[7,8] and Ketjenblack,[9,20] as carbon sources, had been reported on the $LiMnPO_4$ modification. We choose ascorbic acid (Vc) as the carbon sources in this paper. The carbon content was ca. 10.7 wt % after annealing at 600 °C in argon. On the one hand, ascorbic acid can provide a carbon source, on the other hand ascorbic acid (Vc) may prevent $LiMnPO_4$ oxidizing. Figure 5 shows the capacity retention of Li/$LiMnPO_4$ cells at room temperature at the 0.1 C. Each cell was charged at a constant current rate of 0.1 C to 4.9 V, kept at 4.9 V until 0.01 C, and then discharged at 0.1 C to 2.5 V. Apparently, the $LiMnPO_4$/C (Sample d′) discharge capacity at room temperature was higher than the pure $LiMnPO_4$ (Sample d). At the same time, $LiMnPO_4$/C (Sample d′) showed a stable discharge capacity after 50 cycles at room temperature. The initial discharge capacities of the $LiMnPO_4$/C (Sample d′) was 125.5 mA h g^{-1} at 0.1 C at room temperature, and the cell maintained most of its initial capacity, retaining 86.7% of the initial capacity after 50 cycles, while the Li/$LiMnPO_4$ cell maintained 65.6% of the initial capacity. We tried to modify other microstructured $LiMnPO_4$ by annealing with ascorbic acid, and carbon was not observed on the surface of microstructured $LiMnPO_4$. It is possible that the sizes of products are too big to be modified by carbon.

In summary, $LiMnPO_4$ nanosquares with the edge size of 800–1000 nm and the thickness of 50–250 nm were hydrothermally prepared using 1.0 g of $Na_4P_2O_7 \cdot 10H_2O$. The nanosquares show favorable overall capacities. Subsequently, the $LiMnPO_4$ nanosquares were annealed with ascorbic acid (Vc) at 600 °C to prepare the $LiMnPO_4$/C nanocomposites. The electrochemical performances of $LiMnPO_4$ and $LiMnPO_4$/C at 0.1 C demonstrated first-run discharge capacities at 81.6 and 125.5 mA h g^{-1}, respectively. $LiMnPO_4$/C maintained a stable discharge capacity at 108.8 mA h g^{-1} after 50 circles under 0.1 C. In addition, spindles, bows, and cubes composed of nanosquares have also been prepared varying the amount of $Na_4P_2O_7 \cdot 10H_2O$ from 0 to 0.4 g. Their electrochemical capacities were lower than the $LiMnPO_4$ nanosquares, and this may be caused by their large size. We considered that $Na_4P_2O_7 \cdot 10H_2O$ is as the dispersant for tailoring the preparation of small particles of $LiMnPO_4$. Further work for tailoring the preparation of small particles of $LiMnPO_4$ and surface modifying has potentially considerable prospect.

We thank the financial support from the National Nature Science Fund of China (No. 91022033) and the 973 Project of China (No. 2011CB935900).

References and Notes

1 T. Shiratsuchi, S. Okada, T. Doi, J.-i. Yamaki, *Electrochim. Acta* **2009**, *54*, 3145.
2 D. Choi, D. Wang, I.-T. Bae, J. Xiao, Z. Nie, W. Wang, V. V. Viswanathan, Y. J. Lee, J.-G. Zhang, G. L. Graff, Z. Yang, J. Liu, *Nano Lett.* **2010**, *10*, 2799.
3 C. Delacourt, P. Poizot, M. Morcrette, J.-M. Tarascon, C. Masquelier, *Chem. Mater.* **2004**, *16*, 93.
4 T. Drezen, N.-H. Kwon, P. Bowen, I. Teerlinck, M. Isono, I. Exnar, *J. Power Sources* **2007**, *174*, 949.
5 D. Wang, H. Buqa, M. Crouzet, G. Deghenghi, T. Drezen, I. Exnar, N.-H. Kwon, J. H. Miners, L. Poletto, M. Grätzel, *J. Power Sources* **2009**, *189*, 624.
6 S.-M. Oh, S. W. Oh, S.-T. Myung, S.-M. Lee, Y.-K. Sun, *J. Alloys Compd.* **2010**, *506*, 372.
7 S.-M. Oh, S.-W. Oh, C.-S. Yoon, B. Scrosati, K. Amine, Y.-K. Sun, *Adv. Funct. Mater.* **2010**, *20*, 3260.
8 Z. Bakenov, I. Taniguchi, *Electrochem. Commun.* **2010**, *12*, 75.
9 Z. Bakenov, I. Taniguchi, *J. Power Sources* **2010**, *195*, 7445.
10 D. Rangappa, K. Sone, M. Ichihara, T. Kudo, I. Honma, *Chem. Commun.* **2010**, *46*, 7548.
11 P. Barpanda, K. Djellab, N. Recham, M. Armand, J.-M. Tarascon, *J. Mater. Chem.* **2011**, *21*, 10143.
12 Y. Wang, Y. Yang, Y. Yang, H. Shao, *Solid State Commun.* **2010**, *150*, 81.
13 Y. Wang, Y. Yang, Y. Yang, H. Shao, *Mater. Res. Bull.* **2009**, *44*, 2139.
14 A. F. Liu, Z. H. Hu, Z. B. Wen, L. Lei, J. An, *Ionics* **2010**, *16*, 311.
15 H. Ji, G. Yang, H. Ni, S. Roy, J. Pinto, X. F. Jiang, *Electrochim. Acta* **2011**, *56*, 3093.
16 B. Milke, P. Strauch, M. Antonietti, C. Giordano, *Nanoscale* **2009**, *1*, 110.
17 H. Fang, L. Li, Y. Yang, G. Yan, G. Li, *Chem. Commun.* **2008**, 1118.
18 A. R. Studart, E. Amstad, L. J. Gauckler, *Langmuir* **2007**, *23*, 1081.
19 S. K. Martha, B. Markovsky, J. Grinblat, Y. Gofer, O. Haik, E. Zinigrad, D. Aurbach, T. Drezen, D. Wang, G. Deghenghi, I. Exnar, *J. Electrochem. Soc.* **2009**, *156*, A541.
20 J. Xiao, W. Xu, D. Choi, J.-G. Zhang, *J. Electrochem. Soc.* **2010**, *157*, A142.
21 Supporting Information is available electronically on the CSJ-Journal Web site, http://www.csj.jp/journals/chem-lett/index.html.

